IEEE Access
Multidisciplinary ⋮ Rapid Review ⋮ Open Access Journal

Received April 29, 2020, accepted May 13, 2020, date of publication May 19, 2020, date of current version June 3, 2020.

Digital Object Identifier 10.1109/ACCESS.2020.2995723

Circular Polarization Diversity Implementation for Correlation Reduction in Wideband Low-Cost Multiple-Input-Multiple-Output Antenna

UBAID ULLAH[1], (Member, IEEE), MUATH AL-HASAN[1], (Senior Member, IEEE), SLAWOMIR KOZIEL[2,3], (Senior Member, IEEE), AND ISMAIL BEN MABROUK[1], (Senior Member, IEEE)

[1]Networks and Communication Engineering Department, Al Ain University, Abu Dhabi 112612, United Arab Emirates
[2]Engineering Optimization and Modeling Center, Reykjavik University, 101 Reykjavik, Iceland
[3]Faculty of Electronics, Telecommunications and Informatics, Gdańsk University of Technology, 80-233 Gdańsk, Poland

Corresponding author: Ubaid Ullah (ubaid.ullah@aau.ac.ae)

This work was supported in part by the Abu Dhabi Department of Education and Knowledge (ADEK) Award for Research Excellence, in 2019, under Grant AARE19-245, in part by The Icelandic Centre for Research (RANNIS) under Grant 206606051, and in part by the National Science Centre of Poland under Grant 2017/27/B/ST7/00563.

ABSTRACT In this paper, a multiple-input-multiple-output (MIMO) antenna featuring circular polarization diversity, and designed on a common coplanar ground is presented. The proposed antenna design utilizes a coplanar waveguide (CPW) feeding technique with three parallel coplanar ground planes, and two feedlines in-between. For circular polarization (CP), quasi-loops are created by etching slots on the outermost ground planes. With this configuration, circular polarization diversity is induced in the MIMO antenna with the left-hand CP (LHCP) from one antenna and the right-hand CP (RHCP) from the other. The total footprint of the antenna radiator is only $0.78\lambda_0 \times 0.55\lambda_0 = 0.42\lambda_o^2$. Experimental results show perfectly overlapping impedance and axial ratio bandwidths of 39.3% (4.5 GHz to 6.7 GHz). In addition, average in-band isolation $|S_{21}| \leq -15$ dB without any added complexity or active circuit elements. The peak realized gain of the antenna is 5.8 dBic with broadside radiation pattern in the +z- direction and envelope correlation coefficient (ECC) of 0.005. The antenna is suitable for multiple applications in the C-band that includes WLAN (5 GHz, 5.2 GHz and 5.8 GHz) and WiMAX (5.5 GHz).

INDEX TERMS MIMO antenna, circular polarization, polarization diversity, coplanar waveguide, circuit optimization.

I. INTRODUCTION

Multiple-input-multiple-output (MIMO) technology significantly improve the capacity of wireless communication systems [1]–[3]. This technology has the ability to cater the need of high data rates without additional power requirements and therefore, has emerged as a propitious choice for modern wireless communications. MIMO systems generally employ more than one antenna at the transmitting and the receiving ends for sending and receiving multiple signals over the same channel. This approach effectively enhances the channel capacity, spectral efficiency and radio communication links, especially in a rich multipath environment [4], [5]. Giving to the relation $K = \min(M,N)$ for a $M \times N$ MIMO antenna, the signal throughput of a communication system can be improved up to K times only with the low level of correlation between the closely spaced antennas. [6]. In particular, the isolation between the antennas in a compact system is a serious concern due to its adverse effects on the system performance. To fulfill a continuous increase of demands for high capacity, compact size, and to mitigate the issues pertinent to antenna correlation, extensive research efforts have been focused towards the improvement and implementation of techniques aiming at further performance enhancement of the MIMO systems.

Various isolation techniques and decoupling circuits can be applied to reduce the antenna correlation [7]. Among them, one option is the spatial diversity technique, in which antennas with the same radiation characteristics are placed at some distance from each other. It is a common and effective

The associate editor coordinating the review of this manuscript and approving it for publication was Kwok L. Chung.

way of isolating the antennas, which is however hindered in size-constrained scenarios. Similarly, using other isolation techniques, such as parasitic elements, neutralization lines, orthogonal feeding of the antennas, electromagnetic bandgap (EBG) structures and decoupling circuits adds to the detrimental circuit complexity and the overall size of the antenna [8], [9]. In addition to multiple antennas used in the MIMO systems, polarization of the antenna is yet another crucial consideration in improving the signal integrity of the communication system [10]. In relation to this, antenna polarization diversity techniques were considered to attain lower level of far-field correlation between the antennas and rendering a chance to establish parallel sub-channels. In [11]–[13], MIMO antennas with polarization diversity were presented, in which linearly (horizontally and vertically) polarized antennas were deployed. Unfortunately, with the increasing pervasion of wireless technology and modern infrastructure, linearly polarized (LP) antennas are prone to high path losses, absorption losses, Faradays rotation effects and increased sensitivity to alignment between transmitting and receiving antennas. On the other hand, circular polarization (CP) exhibits certain advantages in terms of signal propagation. Some notable features of CP include reduced multipath effects and low sensitivity to spatial alignment between the antennas at the transmitting and receiving end of the system [14]–[18].

In [19], it has been shown that MIMO antenna with dual CP or CP diversity can dramatically improve the system capacity by exploiting low far-field correlations, especially in a dense multipath environment. Several MIMO antennas adopting the CP polarization diversity technique have been proposed [20]–[22]. The dual-polarized features are achieved using added circuit elements such as hybrid couplers and diodes. Apart from the complexity of the circuit, these components need additional DC-biasing which adds to the cost, physical size and implementation of the antenna in consumer electronics. Moreover, these antennas do not comply with the bandwidth requirement of modern communication systems and their complex excitation mechanisms lead to reduced polarization purity. Polarization-reconfigurable structures are another way of reducing the correlation between the antennas. However, this approach is not straightforward to implement and involves high power circuit elements and complex feeding mechanisms. The benefits of this approach are contingent upon certain conditions which makes it less attractive in the context of size, cost-effectiveness and power requirements [23].

In contrast to the aforementioned MIMO structures, in this paper, a simple technique for exploiting circular polarization diversity is presented, which enables reduced cost and implementation complexity. The proposed antenna is comprised of three parallel placed coplanar ground plane with two microstrip feedline in-between the ground planes. Two quasi-loops current paths for the travelling wave are generated in the outermost ground planes which generates CP with opposite sense of polarization. The symmetry of the inner ground plane is broken along the longitudinal axis of the feeding line. With this configuration of the antenna, an inverse correlation between the radiated field is engineered which leads to low level of envelop correlation coefficient (ECC) of 0.005. Furthermore, the antenna maintains wide impedance and axial-ratio bandwidths of 39.3% (4.5 GHz to 6.7 GHz). Moreover, the proposed antenna can be operated with bidirectional (indoor applications, such as tunnels, subways etc.) as well as unidirectional radiation pattern characteristics in the C-band. The major contribution of the work include: (i) development of a new circularly polarized MIMO antenna in a parallel configuration, excited by a coplanar waveguide feed with a common coplanar ground plane; (ii) adaptation of circular polarization diversity for reducing the far field correlation between the two closely spaced antennas; (iii) demonstration (both numerical and experimental) of successful circular polarization diversity in the MIMO antenna without any added circuit element for altering the sense of polarization; (iv) achieving high performance with topologically simple, small size and low-cost structure without involving any additional isolation technique.

II. ANTENNA DESIGN AND MIMO CONFIGURATION

A. ANTENNA DESIGN

The geometrical configuration and parameterized top view of the proposed antenna is shown in Fig. 1. The CP MIMO antenna is comprised of two closely spaced mirrored wide-slot type antennas fed by a coplanar waveguide with a common middle ground plane. The antenna is printed on the FR4 substrate ($\varepsilon_r = 4.4$, $h = 1.5$ mm, $\tan\delta = 0.02$) with the external dimensions of $W_s \times L_s = 0.78\lambda_0 \times 0.55\lambda_0$. The size of the antenna is calculated in free-space wavelength at the lowest operating frequency of the antenna. The MIMO antenna arrangement is initiated by designing a wideband right-hand circularly polarized (RHCP) antenna fed by a single-port 50-Ohm coplanar waveguide (CPW) with a coplanar gap g. CP is induced by etching a slot of modified rectangular-shape in the coplanar ground plane (CG1) which forms a quasi-loop path for the current flow. The middle ground plane (CG2), is made asymmetric along the longitudinal axis of the feeding line. To realize MIMO operation, the geometry of the slotted ground plane (CG1) is mirrored and placed coplanar to the asymmetrical ground plane (CG2). By mirroring the slot topology (CG3), the surface current rotation on the quasi-loop is phase-shifted by 180-degrees. This leads to exciting left-hand circular polarization (LHCP). Further details on the design evolution and operating mechanism of the antenna are explained in the next section.

B. ANTENNA EVOLUTION

The design process of the proposed CP MIMO antenna involves several stages. In the first stage, a rectangular slot is etched in the coplanar ground plane to the left of the microstrip line. This creates a current path along x and y-direction. The impedance matching at this stage shows a

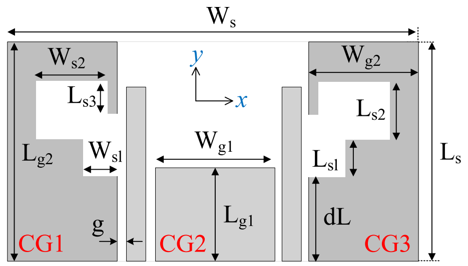

FIGURE 1. Geometry of the proposed CP MIMO antenna with polarization diversity.

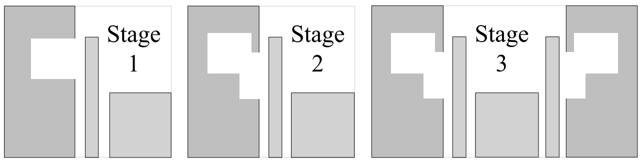

FIGURE 2. CP MIMO antenna evolution stages.

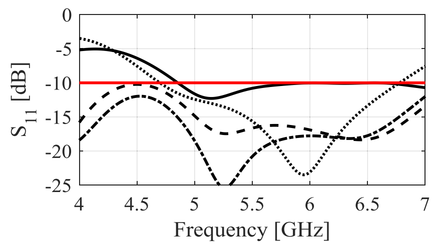

FIGURE 3. S-parameters through design stages: Stage 1 (–), Stage 2 (–), Stage 3 (…), and S_{12} (-.-).

resonance in the 5 GHz band but with poor matching. Also, the AR response in Stage 1 (Fig. 4) shows some circular polarization, which is due to the field components forming a partial loop along W_{s2} and L_{s2} (See Fig.1). In Stage 2, the slot length is extended in the –*y*-direction and a stub is protruded along the length of the CPW feedline. This result in lengthening the current path by increasing the perimeter of the loop. Following the preliminary design, the antenna is optimized in two steps. First, the impedance bandwidth is optimized with the objective being maximization of the operating impedance bandwidth. In the second step, the antenna is re-optimized to minimize its axial ratio (AR). A penalty factor is added to the cost function to enforce the condition $|S_{11}| \leq -10$ dB over the operating frequency range. The single element antenna operates in the frequency range of 3.1 GHz to 7.2 GHz with RHCP. In the third design stage, the MIMO configuration is implemented as depicted in Fig. 2. A second microstrip line extension is added to the right of the ground plane (CG2) with the coplanar gap *g*, and the plane of the CG1 is altered and CG3 is formed. Note that at this stage, the dimensions of all the geometrical parameters are the same as that of the single element.

The small spatial distance between the two resonating elements leads to high mutual coupling, which degrades the electrical characteristics of the antenna. To operate the antenna

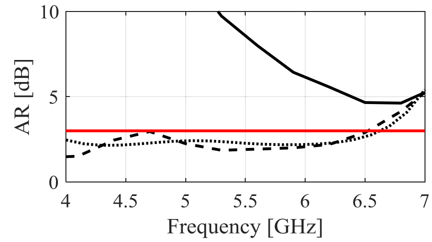

FIGURE 4. AR through design stages: Stage 1 (–), Stage 2 (–), and Stage 3 (…..).

TABLE 1. List of geometrical parameters in Millimeter (mm).

Parameter	Value	Parameter	Value	Parameter	Value
L_s	36.44	L_{sl}	5.3	L_{s2}	9.39
W_s	51.7	W_{sl}	4.64	W_{s2}	10.89
L_{g1}	12.61	L_m	26.41	L_c	22.0
L_{g2}	38.44	W_{g1}	18.0	W_{g2}	12.86
g	0.40	W_m	3.2	L_{s3}	4.96
dL	9.9	W_{s3}	2.0		

effectively, three further optimization steps are performed, aiming at improvement of antenna impedance bandwidth, AR and isolation ($|S_{12}|$), respectively. The S-parameter and axial ratio performance through the development stages are shown in Figs. 3 and 4, respectively. The scattering parameters show that the antenna impedance bandwidth has been reduced in the MIMO configuration. The average isolation (S_{12}) between the two radiators is roughly −16 dB, and it is attained without involving any special isolation improvement techniques. The final geometrical parameters are listed in Table 1.

C. ANTENNA OPERATING MECHNISAM AND POLARIZATION DIVERSITY

The circular polarization operation mechanism is explained using the magnetic surface current distribution illustrated in Fig. 5. The current distribution at the center frequency of the MIMO antenna in Fig. 5(a) corresponds to the RHCP, whereas Fig. 5(b) shows the LHCP. Note that the impedance bandwidth and axial ratio of the single-element design shown in Fig. 3 and Fig. 4 are wider than for the MIMO design. For the single element, the horizontal current on the asymmetrical ground plane (CG2, cf. Fig. 1) and the vertical current on the microstrip line monopole extension also contribute to the antenna CP bandwidth. In the case of MIMO antenna, the horizontal currents flowing from Port 1 to Port 2 are phase-shifted by 180-degrees. Due to the opposite direction of the current on the edge of the common coplanar ground plane between the two antennas, the out-of-phase radiation under the far-field conditions leads to current cancellation as depicted using X in Fig. 5. As a result, the antenna operating bandwidth is reduced but the isolation between the two antennas is improved at the same time. The size of the middle ground plane along the x-axis and the inherent characteristics of the polarization diversity also adds to the

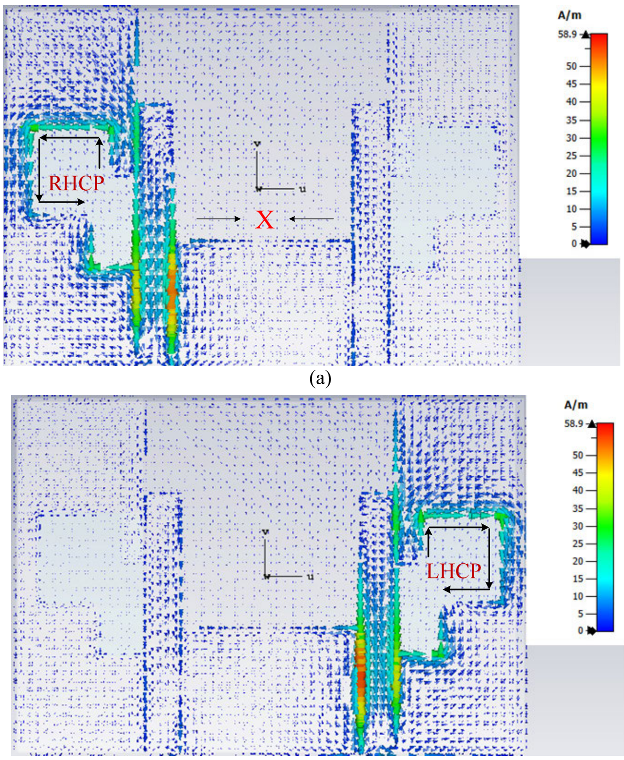

FIGURE 5. Surface current distribution at 5.5 GHz (a) RHCP (b) LHCP.

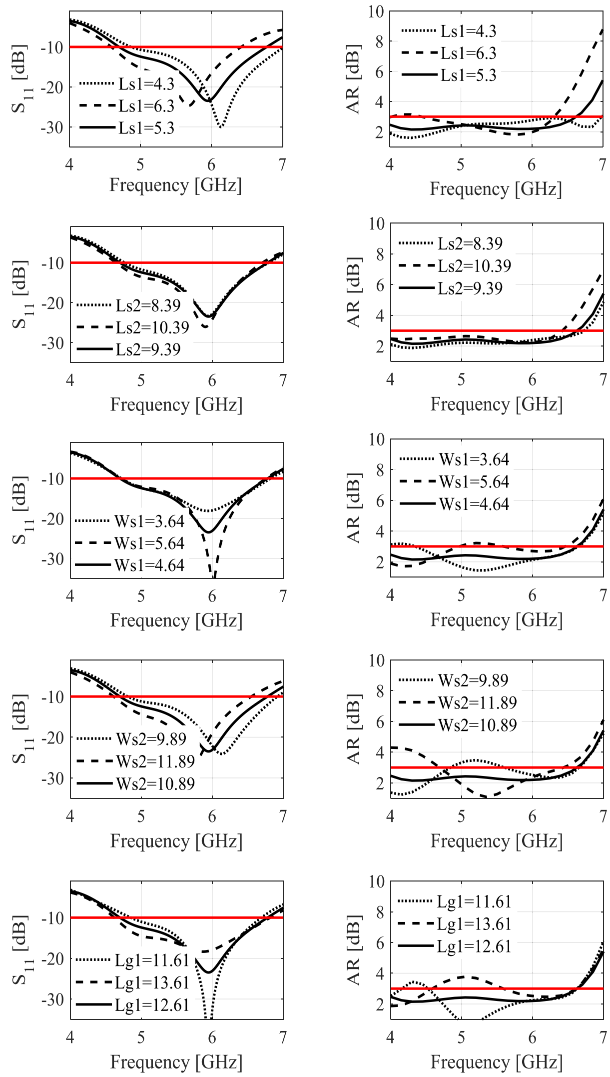

FIGURE 6. Parametric analysis of the proposed MIMO antenna.

level of isolation. The traveling waves quasi-loop current (indicated with arrows) formed at the edges of the modified rectangular slot generates the circular polarization. The counter-clockwise rotation of the fields in the antenna at the left-hand-side (Fig. 5 (a)), radiates RHCP, whereas the antenna on the right-hand-side (Fig. 5 (b)) radiates LHCP.

D. PARAMETRIC ANALYSIS

Parametric analysis of the proposed antenna is performed based on the variable sensitivity. The parameters controlling the size of the slot etched in the coplanar ground plane play a vital role in attaining the wideband CP characteristics.

When the value of the Ls_1 is decreased by 1 mm from the optimized value, the slot size and hence the current path on the edges of the slot is shortened. This results in the upward shift in terms of both S-parameter and AR. Similar behavior is observed when varying L_{s2} which also controls vertical components of the current flowing on the edges of the slot. The horizontal current components are controlled by the width of the slot. Although the impedance bandwidth is not very sensitive to W_{s1}, the AR is affected when it is increased from the optimized value. W_{s2} is one of the critical parameters in tuning the antenna as it controls the perimeter length of the quasi-loop. This can be observed from the S_{11} and AR responses shown in Fig. 6, when the values are altered. By reducing the size of the perimeter, the frequency is shifted upward and vice versa. Another parameter of interest is the common ground plane labeled as L_{g1}. As it can be seen from the impedance matching response, reducing it results in enhancing the antenna impedance matching but the impedance bandwidth is narrowed and the AR bandwidth is almost the same but the value degrades slightly from the 3 dB criterion.

E. PATTERN DIRECTIONALITY

The proposed MIMO antenna can be operated with both bidirectional and unidirectional radiation characteristics. If the antenna is fed using CPW without a ground plane underneath the substrate, the antenna is bidirectional. The radiation pattern of the antenna excited from Port 1 (left-hand-side) is illustrated at 5 GHz and 6 GHz in Fig. 7, which shows RHCP and LHCP in the $\pm z$- direction. Similarly, the antenna excited from Port 2 (right-hand-side), yields LHCP and RHCP in the $\pm$z-direction as depicted in Fig. 8. A minor tilt in the main beam direction is due to the middle asymmetrical ground plane.

Due the asymmetrical configuration of the CPW along the length of the feedline, the current distribution of the

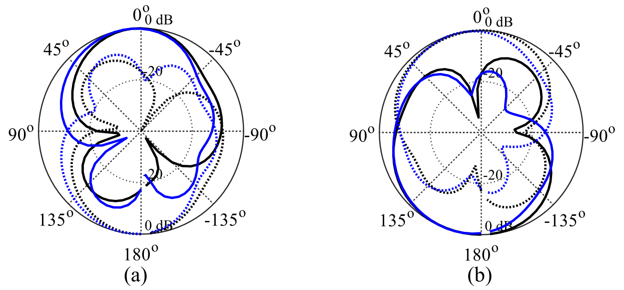

FIGURE 7. Antenna Port 1 radiation pattern without a reflector. RHCP (solid line) and LHCP (dotted line) 5 GHz (black), 6 GHz (blue) (a) *xz*-plane (b) *yz*-plane.

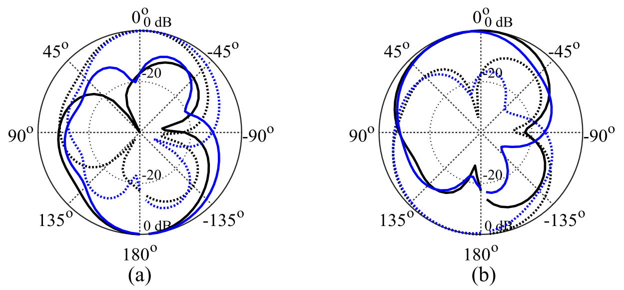

FIGURE 8. Antenna Port 2 radiation pattern without a reflector. LHCP (solid line) and RHCP (dotted line) 5 GHz (black), 6 GHz (blue) (a) *xz*-plane (b) *yz*-plane.

vertical and horizontal ground plane combines to form tilted current that slightly deviates from the main beam direction away from the broadside. It is clearly seen that the antenna has a stable radiation pattern throughout the operating bandwidth with a peak realized of 3.15 dBic. The antenna with bidirectional radiation pattern can be effectively used for various applications such as in tunnels, subways and other indoor environments. As unidirectional radiation characteristics are generally desirable for some applications, therefore, the antenna is also validated for directional pattern. The directionality of the antenna is changed by employing a planar reflector placed at a distance of a quarter wavelength. It is important to mention here that all other geometrical parameters were kept the same as that of the bidirectional design.

III. EXPERIMENTAL VALIDATION AND DISCUSSION

A. S-PARAMETERS AND AXIAL RATIO

The proposed MIMO antenna has been prototyped and characterized in the anechoic chamber of Reykjavik University, Iceland. To achieve unidirectional radiation pattern and to ensure constructive interference between the transmitted and reflected wave, a flat reflector is added at a distance H = 14.5 mm, which is approximately a quarter wavelength at 5.2 GHz. For mechanical support, a rigid plastic of permittivity close to 1 is used. The top view and perspective view of the antenna prototype are shown in Fig. 9.

The measured reflection coefficient of the antenna shown in Fig. 10 (a) indicates that the minimum impedance

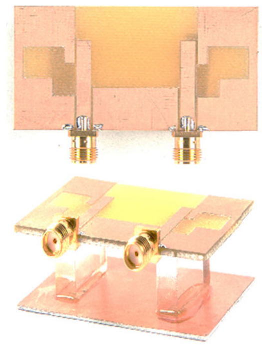

FIGURE 9. Fabricated and characterized antenna prototype.

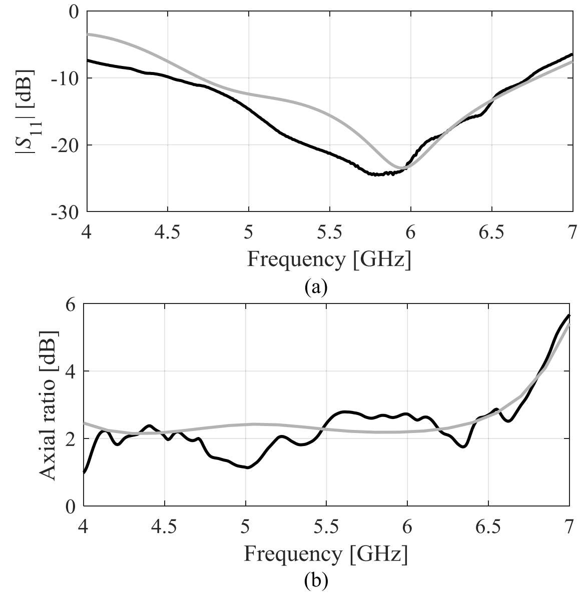

FIGURE 10. Simulated (gray) and measured (black) (a) S_{11} (b) AR.

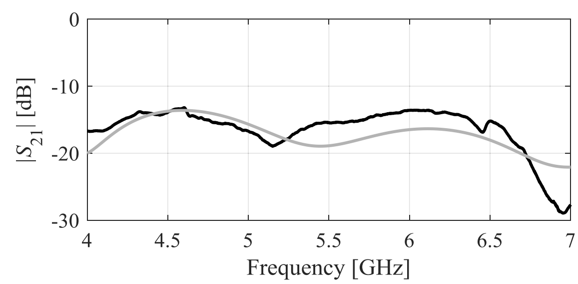

FIGURE 11. Simulated (gray) and measured (black) isolation (S_{12}).

bandwidth of the antenna is 39.3% (4.5 GHz to 6.7 GHz). The AR bandwidth of the antenna covers the same operating range with 100-percent overlap between impedance and AR bandwidth as observed in Fig. 10 (b). Figure 11 shows the simulated and measured $|S_{12}|$. The minimum in-band isolation recorded is approximately −18 dB with average value of −15.5 dB throughout the operating band of the antenna. It should be reminded that this isolation is attained without any additional decoupling elements or employment of isolation improvement technique.

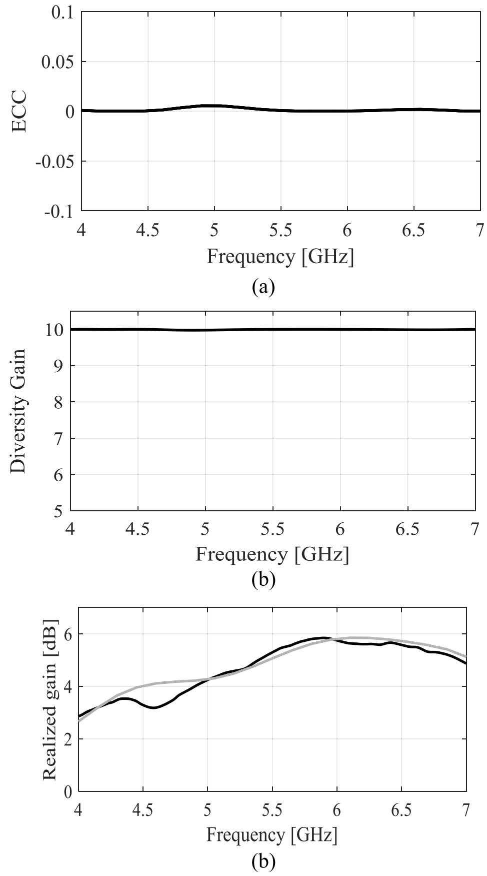

FIGURE 12. (a) Calculated ECC (solid black), (b) Diversity Gain(solid black), (c) Simulated (gray) and measured (black) realized gain.

B. ENVELOPE CORRELATION COEFFICIENT AND DIVERSITY GAIN

ECC is an important parameter that characterizes the performance of the MIMO antenna in terms of correlation between the two antennas. As the channel capacity of a wireless system depends on this performance metrics, the lower the correlation the better the channel capacity and the signal integrity. Here, ECC is evaluated using the far-field radiation patterns as:

$$\rho e = \frac{|\iint_{4\pi} \left[\vec{F}_\iota(\theta,\phi) * \vec{F}_j(\theta,\phi)\right] d\Omega|^2}{\iint_{4\pi} |\vec{F}_\iota(\theta,\phi)|^2 * \iint_{4\pi} \vec{F}_j(\theta,\phi)|^2} \tag{1}$$

$$DG = 10\sqrt{1-|\rho e|^2} \tag{2}$$

The ECC is shown in Fig. 12 (a). The fields radiated by the proposed antenna with polarization diversity are almost entirely uncorrelated due to the opposite sense of rotation. A low level of ECC < 0.005 is observed. The slight shift in the main beam direction (due to the asymmetrical geometry of the CPW) contributes to the low level of correlation between the two antennas. The diversity gain of the antenna is calculated using equation (2) and plotted in Fig. 12 (b). It can be oberved that the proposed antenna has almost maximum diversity gain of 9.997. the low level of ECC and high diversity gain are attributed to the polarization diversity of the proposed antenna.

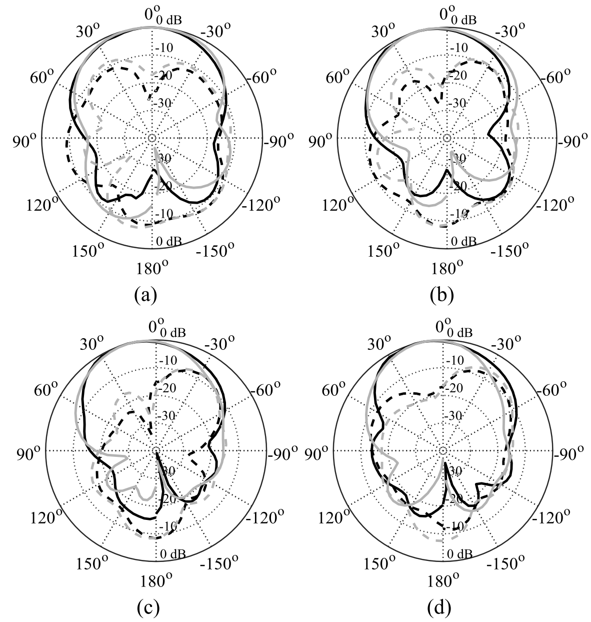

FIGURE 13. Simulated (gray) and measured (black) radiation pattern port 1 – *xz*-plane (a) 5.0 GHz, (b) 5.5 GHz, (c) 6.0 GHz, and (d) 6.5 GHz; Co-pol (solid), and cross-pol (dashed).

C. REALIZED GAIN AND RADIATION PATTERN

The simulated and measured realized gain of the antenna is shown in Fig. 12 (c). The measured peak realized gain is 5.8 dBic with average in-band variation of 1.55 dB. The gain drop at the lower edge of the operating frequency is due to the destructive interference with the reflector. The radiation pattern of the antenna has been measured for both ports.

Figure 13 and Fig. 14 illustrates the pattern in terms of co-polarized and cross-polarized fields for antenna excited from Port 1, in the *xz*-plane and *yz*-plane at four different frequencies. The antenna exhibits a steady radiation pattern in the entire operating band with a difference between co-pol and cross-pol of more than 20 dB in the main beam direction. The slight beam tilt in the main beam direction is due to the asymmetrical configuration of the coplanar waveguide ground planes. This adds to the lower value off ECC, because along with polarization diversity, pattern diversity is induced. For port 1, the main beam direction shift is approximately +10-degrees. The patterns for Port 2 in the *xz*-plane and *yz*-plane are shown in Fig. 15 and Fig. 16 respectively. The shape of the pattern is the same as that of the port 1 in both planes. The tilt in the main beam direction is −10-degrees.

D. ANTENNA EFFICIENCY AND TARC

The antenna total and radiation efficiencies are shown in Fig. 17. The maximum radiation efficiency of the antenna is approximately 92% while the total efficiency more than 86% within the overall operating band. The efficiency graph illustrates that the antenna retains a relatively stable in-band

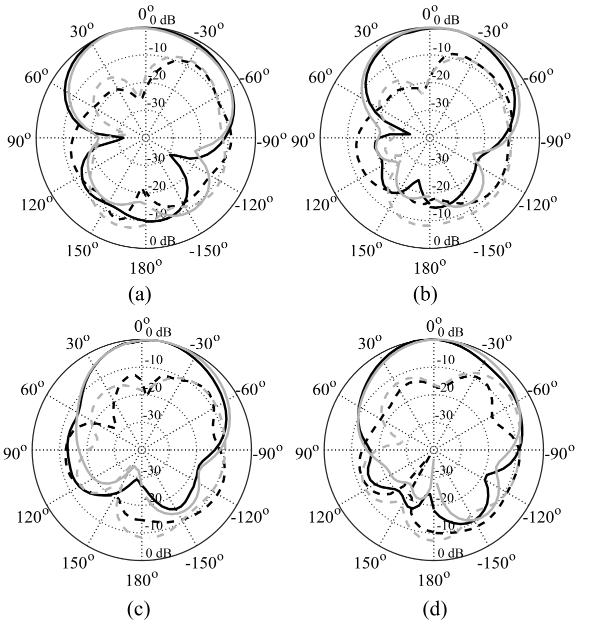

FIGURE 14. **Simulated (gray) and measured (black) radiation pattern port 1 – *yz*-plane (a) 5.0 GHz, (b) 5.5 GHz, (c) 6.0 GHz, and (d) 6.5 GHz; Co-pol (solid), and cross-pol (dashed).**

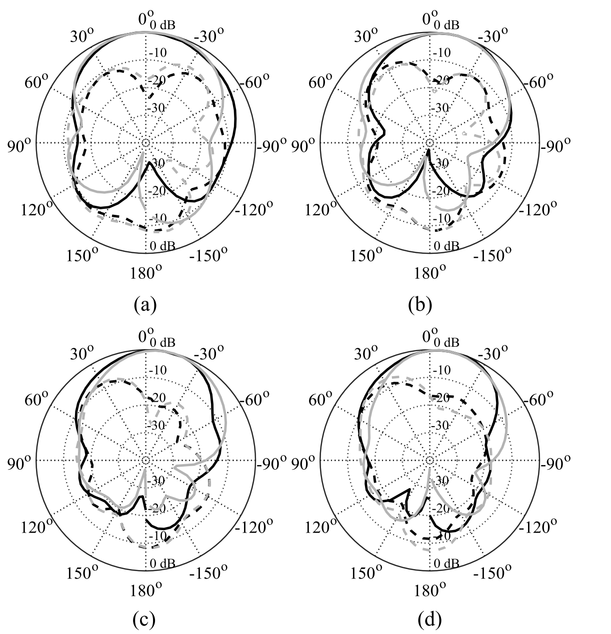

FIGURE 15. **Simulated (gray) and measured (black) radiation pattern port 2 – *xz*-plane (a) 5.0 GHz, (b) 5.5 GHz, (c) 6.0 GHz, and (d) 6.5 GHz; Co-pol (solid), and cross-pol (dashed).**

efficiency. Moreover, to analyze the behavior of the individual port reflected signal, the total active reflection coefficient (TARC) is studied. The calculation of the TARC is carried out according to the technique described in [31] as

$$\Gamma_a^t = \frac{\sqrt{|\left(S_{11} + S_{12}e^{j\theta}\right)|^2 + |(S_{21} + S_{22}e^{j\theta})|^2}}{\sqrt{2}} \tag{3}$$

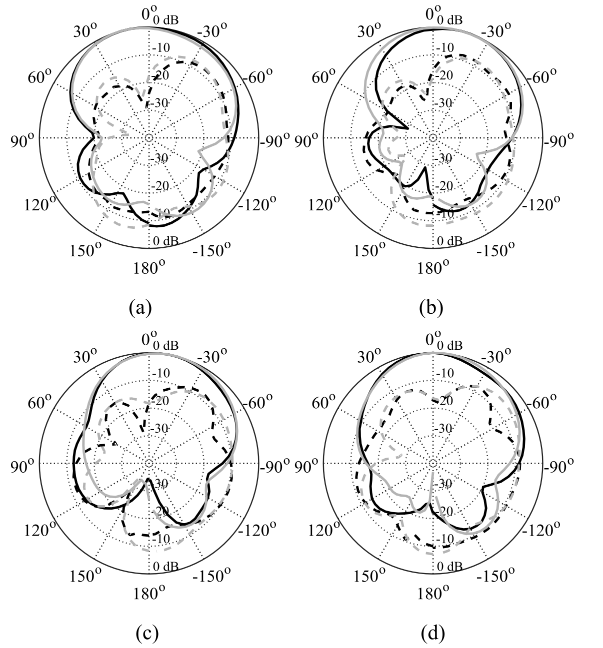

FIGURE 16. **Simulated (gray) and measured (black) radiation pattern port 2 – *yz*-plane (a) 5.0 GHz, (b) 5.5 GHz, (c) 6.0 GHz, and (d) 6.5 GHz; Co-pol (solid), and cross-pol (dashed).**

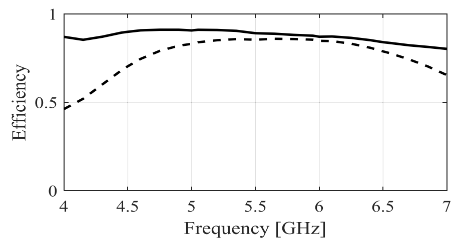

FIGURE 17. **Antenna Radiation (–) and total ((–) efficiency.**

TABLE 2. **Comparison with State-of-The-Art MIMO Antennas.**

Ref	Freq (GHz)	Polarization	Size [L×W×H]	S_{12} (dB)	Gain (dBi)	%AR	%BW
[5]	3.3	LP	50×100×7	25	4	----	28.5
[8]	5.3	LP/CP	29×48×1.6	18	2.85	2.32	16.28
[21]	5.1	CP	32×32×3	20	5	13.7	13.7
[23]	5.5	CP	30×25×1.524	13	~ 4.5	4.7	4.7
[25]	2.4	Dual	38.1×38.1	12	2.79	----	20
[26]	2.4/5.1	LP	77.5×52	15	----	----	8.2
[27]	5.2	CP	36.5×13.2×13.6	22	5.8	18.3	18.3
[28]	2.16	CP	83.8×83.8×15	14.5	7.08	26.45	26.45
[29]	4.2	LP	59.5×59.5×5	15	5.2	--	22.3
[30]	2.4/5.1	LP	180×90×27	27	5	---	25
This work	4.5	CP	36.44×51.714.2	15.5	5.8	39.3	39.3

The phase angle θ of port 2 excitation accounts for port-to-port coupling and also random signal combining.

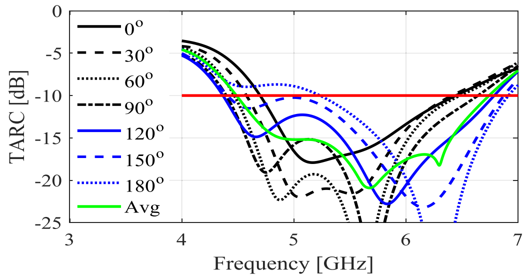

FIGURE 18. TARC calculation for one antenna with constant amplitudes and different phase angles of port 2.

A set of curves is shown in Fig. 18 for different phased signal excitation of Port 2. The curve characteristics changes slightly with the phase change due to the effects of mutual coupling and random phase signals but the impedance bandwidth remains almost intact. The average TARC values indicate that the antenna retains the impedance bandwidth, whereas, in the worst case, the TARC value of less than -8 dB is observed when the signal is 180^0 out of phase.

IV. BENCHMARKING

For benchmarking, the proposed MIMO antenna has been compared with the recent state-of-the-art MIMO antenna designs with polarization diversity, cf. Table 2. It should be emphasized that, to date, there is a limited amount of work published on the antenna with CP diversity. The comparison is carried out in terms of the type of polarization, isolation, antenna footprint, gain, impedance bandwidth, and AR bandwidth. The antenna operating frequencies are also included in the table for fair comparison. The size of the antennas are shown in millimeter. As it can be observed from the data in Table 2, the proposed design is competitive with respect to almost all considered performance figures. In particular, in comparison to the CP designs reported in [22], [24], [27], [28], the proposed antenna is better in certain aspects including the impedance bandwidth and the AR bandwidth. It should be emphasized that apart from the gain of the antenna, the impedance bandwidth and AR bandwidth of the proposed MIMO antenna outperform all the benchmark designs reported in the recent literature.

V. CONCLUSION

In this communication, a new design of circularly polarized wideband MIMO antenna with polarization diversity has been presented. The MIMO antenna is developed from a single-point coplanar waveguide fed wideband CP antenna. For the single element design, one-side of the coplanar ground plane is systematically modified to induce circular polarization, whereas the other side of the coplanar ground plane is made asymmetric along the length of the feedline. For MIMO implementation, another feedline is added next to the asymmetrical ground plane in a parallel configuration, and the position of the modified ground plane is switched to alter the sense of polarization. With this formation of the radiators, the multi-element antenna features two senses of circular polarization which renders polarization diversity without any additional circuit element. The design has been prototyped and validated experimentally. The inverse correlation between the radiated fields result in a low level ECC < 0.005. Moreover, a stable radiation (bi-directional/unidirectional) characteristic in the broadside direction, wide impedance and AR bandwidth, relatively high gain and compact size is realized.

ACKNOWLEDGMENT

The authors would like to thank Dassault Systemes, France, for making CST Microwave Studio available.

REFERENCES

[1] Y. Yang, Q. Chu, and C. Mao, "Multiband MIMO antenna for GSM, DCS, and LTE indoor applications," *IEEE Antennas Wireless Propag. Lett.*, vol. 15, pp. 1573–1576, 2016.
[2] G.-S. Lin, C.-H. Sung, J.-L. Chen, L.-S. Chen, and M.-P. Houng, "Isolation improvement in UWB MIMO antenna system using carbon black film," *IEEE Antennas Wireless Propag. Lett.*, vol. 16, pp. 222–225, 2017.
[3] M. Al-Hasan, I. Ben Mabrouk, E. R. F. Almajali, M. Nedil, and T. A. Denidni, "Hybrid isolator for mutual-coupling reduction in millimeter-wave MIMO antenna systems," *IEEE Access*, vol. 7, pp. 58466–58474, 2019.
[4] M. A. Ul Haq and S. Koziel, "Feedline alterations for optimization-based design of compact super-wideband MIMO antennas in parallel configuration," *IEEE Antennas Wireless Propag. Lett.*, vol. 18, no. 10, pp. 1986–1990, Oct. 2019.
[5] H. T. Chattha, "4-port 2-element MIMO antenna for 5G portable applications," *IEEE Access*, vol. 7, pp. 96516–96520, 2019.
[6] S. Zhang, K. Zhao, Z. Ying, and S. He, "Investigation of diagonal antenna-chassis mode in mobile terminal LTE MIMO antennas for bandwidth enhancement," *IEEE Antennas Propag. Mag.*, vol. 57, no. 2, pp. 217–228, Apr. 2015.
[7] I. Nadeem and D.-Y. Choi, "Study on mutual coupling reduction technique for MIMO antennas," *IEEE Access*, vol. 7, pp. 563–586, 2019.
[8] Y. Sharma, D. Sarkar, K. Saurav, and K. V. Srivastava, "Three-element MIMO antenna system with pattern and polarization diversity for WLAN applications," *IEEE Antennas Wireless Propag. Lett.*, vol. 16, pp. 1163–1166, 2017.
[9] A. Boukarkar, X. Q. Lin, Y. Jiang, L. Y. Nie, P. Mei, and Y. Q. Yu, "A miniaturized extremely close-spaced four-element dual-band MIMO antenna system with polarization and pattern diversity," *IEEE Antennas Wireless Propag. Lett.*, vol. 17, no. 1, pp. 134–137, Jan. 2018.
[10] P. Kyritsi, D. C. Cox, R. A. Valenzuela, and P. W. Wolniansky, "Effect of antenna polarization on the capacity of a multiple element system in an indoor environment," *IEEE J. Sel. Areas Commun.*, vol. 20, no. 6, pp. 1227–1239, Aug. 2002.
[11] H. Huang, Y. Liu, and S. Gong, "A novel dual-broadband and dual-polarized antenna for 2G/3G/LTE base stations," *IEEE Trans. Antennas Propag.*, vol. 64, no. 9, pp. 4113–4118, Sep. 2016.
[12] C.-Y. Chiu, J.-B. Yan, and R. D. Murch, "Compact three-port orthogonally polarized MIMO antennas," *IEEE Antennas Wireless Propag. Lett.*, vol. 6, pp. 619–622, Dec. 2007.
[13] U. Ullah and S. Koziel, "Design and optimization of a novel miniaturized low-profile circularly polarized wide-slot antenna," *J. Electromagn. Waves Appl.*, vol. 32, no. 16, pp. 2099–2109, Nov. 2018.
[14] H. H. Tran and T. T. Le, "Ultrawideband, high-gain, high-efficiency, circularly polarized archimedean spiral antenna," *AEU-Int. J. Electron. Commun.*, vol. 109, pp. 1–7, Sep. 2019.
[15] P. Mohammadi, M. Rezvani, and T. Siahy, "A circularly polarized wide-band magneto-electric dipole antenna with simple structure for BTS applications," *AEU-Int. J. Electron. Commun.*, vol. 105, pp. 92–97, Jun. 2019.
[16] U. Ullah, I. B. Mabrouk, and S. Koziel, "A compact circularly polarized antenna with directional pattern for wearable off-body communications," *IEEE Antennas Wireless Propag. Lett.*, vol. 18, no. 12, pp. 2523–2527, Dec. 2019.

[17] N. Hussain, H. H. Tran, and T. T. Le, "Single-layer wideband high-gain circularly polarized patch antenna with parasitic elements," *AEU-Int. J. Electron. Commun.*, vol. 113, Jan. 2020, Art. no. 152992.
[18] R. Kumar, S. R. Thummaluru, and R. K. Chaudhary, "Improvements in Wi-MAX reception: A new dual-mode wideband circularly polarized dielectric resonator antenna," *IEEE Antennas Propag. Mag.*, vol. 61, no. 1, pp. 41–49, Feb. 2019.
[19] P.-Y. Qin, Y. J. Guo, and C.-H. Liang, "Effect of antenna polarization diversity on MIMO system capacity," *IEEE Antennas Wireless Propag. Lett.*, vol. 9, pp. 1092–1095, 2010.
[20] Z.-X. Liang, D.-C. Yang, X.-C. Wei, and E.-P. Li, "Dual-band dual circularly polarized microstrip antenna with two eccentric rings and an arc-shaped conducting strip," *IEEE Antennas Wireless Propag. Lett.*, vol. 15, pp. 834–837, 2016.
[21] D. S. Chandu and S. S. Karthikeyan, "A novel broadband dual circularly polarized microstrip-fed monopole antenna," *IEEE Trans. Antennas Propag.*, vol. 65, no. 3, pp. 1410–1415, Mar. 2017.
[22] H. H. Tran, N. Hussain, and T. T. Le, "Low-profile wideband circularly polarized MIMO antenna with polarization diversity for WLAN applications," *AEU-Int. J. Electron. Commun.*, vol. 108, pp. 172–180, Aug. 2019.
[23] S. Karamzadeh, V. Rafii, H. Saygin, and M. Kartal, "Polarisation diversity cavity back reconfigurable array antenna for C-band application," *IET Microw., Antennas Propag.*, vol. 10, no. 9, pp. 955–960, 2016.
[24] J. Malik, A. Patnaik, and M. V. Kartikeyan, "Novel printed MIMO antenna with pattern and polarization diversity," *IEEE Antennas Wireless Propag. Lett.*, vol. 14, pp. 739–742, 2015.
[25] H. Li, S. Sun, B. Wang, and F. Wu, "Design of compact single-layer textile MIMO antenna for wearable applications," *IEEE Trans. Antennas Propag.*, vol. 66, no. 6, pp. 3136–3141, Jun. 2018.
[26] J. Deng, J. Li, L. Zhao, and L. Guo, "A dual-band inverted-F MIMO antenna with enhanced isolation for WLAN applications," *IEEE Antennas Wireless Propag. Lett.*, vol. 16, pp. 2270–2273, 2017.
[27] U. Ullah, I. B. Mabrouk, and S. Koziel, "Enhanced-performance circularly polarized MIMO antenna with Polarization/Pattern diversity," *IEEE Access*, vol. 8, pp. 11887–11895, 2020.
[28] M. Ameen, O. Ahmad, and R. K. Chaudhary, "Wideband circularly-polarised high-gain diversity antenna loaded with metasurface reflector for small satellite applications," *Electron. Lett.*, vol. 55, no. 15, pp. 829–831, Jul. 2019.
[29] L. Si, H. Jiang, X. Lv, and J. Ding, "Broadband extremely close-spaced 5G MIMO antenna with mutual coupling reduction using metamaterial-inspired superstrate," *Opt. Express*, vol. 27, no. 3, pp. 3472–3482, 2019.
[30] M. Rezvani and Y. Zehforoosh, "A dual-band multiple-input multiple-output microstrip antenna with metamaterial structure for LTE and WLAN applications," *AEU-Int. J. Electron. Commun.*, vol. 93, pp. 277–282, Sep. 2018.
[31] S. H. Chae, S.-K. Oh, and S.-O. Park, "Analysis of mutual coupling, correlations, and TARC in WiBro MIMO array antenna," *IEEE Antennas Wireless Propag. Lett.*, vol. 6, pp. 122–125, 2007.

UBAID ULLAH (Member, IEEE) received the M.Sc. and Ph.D. degrees in electrical and electronic engineering from the Universiti Sains Malaysia, in 2013 and 2017, respectively. He was with the Engineering Optimization and Modeling Center, School of Science and Engineering, Reykjavik University, Iceland, from 2017 to 2019. He is currently affiliated with Al Ain University, Abu Dhabi, United Arab Emirates. His research interests include antenna theory, small antennas, antenna polarization, dielectric resonators, waveguides, millimeter-wave antenna designs, multiple-input multiple-output (MIMO) antenna systems, EM-simulation-driven design, numerical analysis, and microwave circuit design and optimization. He received the Prestigious Global Fellowship and the Outstanding Student Award.

MUATH AL-HASAN (Senior Member, IEEE) received the B.A.Sc. degree in electrical engineering from the Jordan University of Science and Technology, Jordan, in 2005, the M.A.Sc. degree in wireless communications from Yarmouk University, Jordan, in 2008, and the Ph.D. degree in telecommunication engineering from the Institut National de la Recherche Scientifique (INRS), Université du Québec, Canada, in 2015. From 2013 to 2014, he was with Planets Inc., San Francisco, CA, USA. In May 2015, he joined Concordia University, Canada, as a Postdoctoral Fellowship. He is currently an Assistant Professor with Al Ain University, United Arab Emirates. His research interests include antenna design at millimeter-wave and terahertz frequencies, electromagnetic bandgap (EBG) structures, and channel measurements in multiple-input and multiple-output (MIMO) systems.

SLAWOMIR KOZIEL (Senior Member, IEEE) received the M.Sc. and Ph.D. degrees in electronic engineering from the Gdańsk University of Technology, Poland, in 1995 and 2000, respectively, and the M.Sc. degree in theoretical physics and the M.Sc. and Ph.D. degrees in mathematics from the University of Gdańsk, Poland, in 2000, 2002, and 2003, respectively. He is currently a Professor with the School of Science and Engineering, Reykjavik University, Iceland. His research interests include CAD and modeling of microwave and antenna structures, simulation-driven design, surrogate-based optimization, space mapping, circuit theory, analog signal processing, evolutionary computation, and numerical analysis.

ISMAIL BEN MABROUK (Senior Member, IEEE) received the B.A.Sc. and M.A.Sc. degrees in electrical engineering from the University of Lille, Lille, France, in 2006 and 2007, respectively, and the Ph.D. degree in electrical engineering from the University of Quebec, Canada, in 2012. From 2007 to 2009, he was with Huawei Technologies, Paris, France. In 2012, he joined the Wireless Devices and Systems (WiDeS) Group, University of Southern California, Los Angeles, CA, USA. He is currently an Assistant Professor with the Al Ain University of Science and Technology, Abu Dhabi, United Arab Emirates. His research interests include propagation studies for multiple-input and multiple-output (MIMO) systems, measurement campaigns in special environments, WBAN, and antenna design at the millimiter-wave and terahertz frequencies.